Conformational Dynamics of Photoexcited Conjugated Molecules

S. Tretiak,* A. Saxena, R. L. Martin, and A. R. Bishop

Theoretical Division and Center for Nonlinear Studies, Los Alamos National Laboratory, Los Alamos, New Mexico 87545

(Received 14 December 2001; published 9 August 2002)

Time-dependent photoexcitation and optical spectroscopy of π-conjugated molecules is described using a new method for the simulation of excited state molecular dynamics in extended molecular systems with sizes up to hundreds of atoms. Applications are made to poly(p-phenylene vinylene) oligomers. Our analysis shows self-trapping of excitations on about six repeat units in the course of photoexcitation relaxation, identifies specific slow (torsion) and fast (bond-stretch) nuclear motions strongly coupled to the electronic degrees of freedom, and predicts spectroscopic signatures of molecular conformations.

DOI: 10.1103/PhysRevLett.89.097402 PACS numbers: 78.66.Qn, 78.55.Kz

The connection between electronic structure and the optical properties of conjugated molecular compounds constitutes a complex and fundamental problem with important technological implications for organic optoelectronic devices [1], as well as in understanding the fundamental properties of soft organic and biological matter [2]. Almost every photochemical, photophysical, or spectroscopic process in these materials involves coupled electron-nuclear structure dynamics. The computational simulation of such phenomena is a very powerful complement to experiment. It allows investigation of details that would be undetected even in many refined experiments: conformational changes, electronic density variations, etc. [3,4]. This becomes vital for understanding such processes as time-dependent photochemical reactions, dynamics of photoexcitations in molecular systems, formation of excitons, polarons, and other quasiparticles which govern the spectroscopic, photo-optical, energy, and charge transport properties of the media [5–7].

The computational machinery for ground-state adiabatic potential surfaces is well developed. On the other hand, calculation of excited states is much more challenging since it requires an expensive multiconfiguration representation [3]. This high demand on computational resources has limited excited state surface calculations to small molecules (5–10 atoms) [8] or to single-point computations, which compute a snapshot of the excited state structure for a given molecular geometry [3].

In this paper we present a new method for the computation of the excited state potential surfaces of large molecular systems (typically nanoscale size) and apply this technique to photoexcitation dynamics in poly(p-phenylene vinylene) (PPV) oligomers [Fig. 1(a)]. This modeling became possible by combining several recent developments. The collective electronic oscillator (CEO) algorithm [9,10] combines semiempirical Hamiltonians with a time-dependent Hartree-Fock formalism, and makes computation of an excited state manifold not substantially more numerically demanding than ground-state calculations. The CEO was successfully appliedto calculate optical properties of a variety of conjugated chromophores such as polymers, dendrimers, donor-acceptor polymers, and biological light-harvesting complexes [9,10].

The CEO approach was used in the past with the intermediate neglect of differential overlap/spectroscopy Hamiltonian, a model parametrized to reproduce vertical excitation energies of small molecules, where it worked quite well. On the other hand, this Hamiltonian works poorly for the ground-state geometries and is suspect when used to determine excited state geometries or dynamics. To avoid this, the CEO previously utilized two Hamiltonians [11,12]: one to calculate the ground state and another to generate the excited state. We have recently shown, however, that other semiempirical Hamiltonians

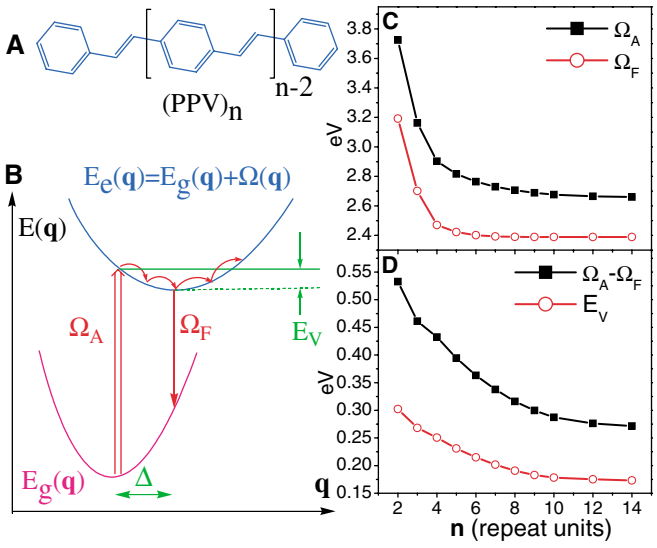

FIG. 1 (color). (a) Geometry of PPV oligomers. (b) Schematic representation of molecular dynamics propagation: The excited state energy $E_e(\mathbf{q})$ as a function of nuclear coordinates $\mathbf{q}$, displacements Δ, vibrational reorganization energy E_v, vertical absorption Ω_A, and fluorescence Ω_F frequencies. Calculated variation of (c) vertical absorption Ω_A and fluorescence Ω_F frequencies, (d) Stokes shift $\Omega_A - \Omega_F$ and vibrational reorganization energy ΔE_v with the number of repeat units in the PPV chain.

 0031-9007/02/89(9)/097402(4)$20.00

designed to reproduce molecular ground-state geometries, energies, and heats of formation [Austin model 1 (AM1) [13] and similar types] yield reasonable estimates of vertical excitation energies, polarizabilities, and excited state adiabatic surfaces [14]. A similar conclusion has been reported in a recent study [15] where the configuration interaction (CI) approach combined with the AM1 has been used to calculate excited state energies and adiabatic surfaces in a number of conjugated oligomers.

Use of a single Hamiltonian for both states [14] results in a significant computational simplification and has made accurate excited state molecular dynamics computations feasible for extended molecular systems. Our method propagates the classical Newtonian equation of motion

$$M_\alpha \frac{\partial^2 \mathbf{q}_\alpha}{\partial t^2} + \beta \frac{\partial \mathbf{q}_\alpha}{\partial t} = \mathbf{F}_\alpha = -\frac{\partial E}{\partial \mathbf{q}_\alpha} \qquad (1)$$

along the trajectory on the excited state molecular potential surface. Here $\mathbf{q}_\alpha$ and M_α represent coordinates and masses of $3N$-6 molecular vibrational normal modes (N being the number of atoms in the molecule), and $E = E_k + E_e$, where E_k is the nuclear kinetic energy and E_e is the excited state potential energy, as shown in Fig. 1(b). The forces $\mathbf{F}_\alpha$ are obtained with the CEO method by computing E as a function of $\mathbf{q}_\alpha$. The computations allow us to follow excited state molecular dynamics in the gas phase with vanishing damping ($\beta = 0$) or motion in an effective viscous medium ($\beta \neq 0$). The latter leads to the excited state optimal geometry [Fig. 1(b)]. Standard Verlet-type numerical integration [16] has been used to propagate Eq. (1) in time. At present the algorithm computes forces $\mathbf{F}_\alpha$ in the excited state with numerical differentiation, as opposed to a more efficient analytical derivative technique which is also possible for the present approach [11,12]. However, implementation of the direct inversion iterative subspace algorithm for calculating the ground-state energy E_g and very efficient Davidson diagonalization techniques for computing excitation frequencies Ω [17] make it possible to follow picosecond dynamics of quite large (100–200 atoms) molecular systems taking into account all ($3N$-6) vibrational degrees of freedom.

We investigated excited state geometries in oligomers of various lengths ($n = 2$–14) of PPV, which is an important material for electronic device applications. The study focuses on the lowest singlet excited state ($1B_u$) of PPV which plays a major role in absorption, photoluminescence, and carrier transport in conjugated systems. The AM1 Hamiltonian [13] has been used in all calculations to obtain ground-state *and* excited state optimal structures and relevant spectroscopic observables. Figures 1(c) and 1(d) show the variation with oligomer size of vertical absorption (computed at the ground-state optimal geometry) and fluorescence (calculated at the excited state optimal geometry) frequencies, Stokes shift, and vibrational reorganization energy [see Fig. 1(b)] for the $1B_u$ transition. The energies of absorption and fluorescence, as expected, are redshifted with increasing oligomer length, saturating to 2.65 and 2.4 eV for long chains, respectively, which compares well with the corresponding experimental values 2.7 and 2.4 eV [18]. The vibrational reorganization energy also decreases with increasing in the chain length, albeit at a slower rate.

The ground-state structure of PPV is not planar [Fig. 2(a)]. Here the energy profile is very shallow with respect to the librational motion; weak perturbations such as impurities and intermolecular interactions may lead to significant torsional disorder. In particular, interaction of the σ bonds results in a structure with the neighboring phenyl-vinyl twisted by $\sim 15°$ in the AM1 geometry, which agrees with x-ray structures reported for $(PPV)_5$ crystals [19]. The situation is very different for the excited state. Here the energy profile is no longer shallow with respect to the torsional motion and has its global minimum at a planar structure shown in Fig. 2(a). An important feature of a conjugated oligomer's geometry is the bond-length alternation due to the uneven distribution of the π electrons over the bonds (Peierls distortion) [3,20]. As shown in Fig. 2(b), the bond-length alternation parameter in the adjacent vinylene linkages of $(PPV)_{14}$ is constant along the chain for the ground-state geometry and noticeably reduced in the middle of the molecule for the excited state

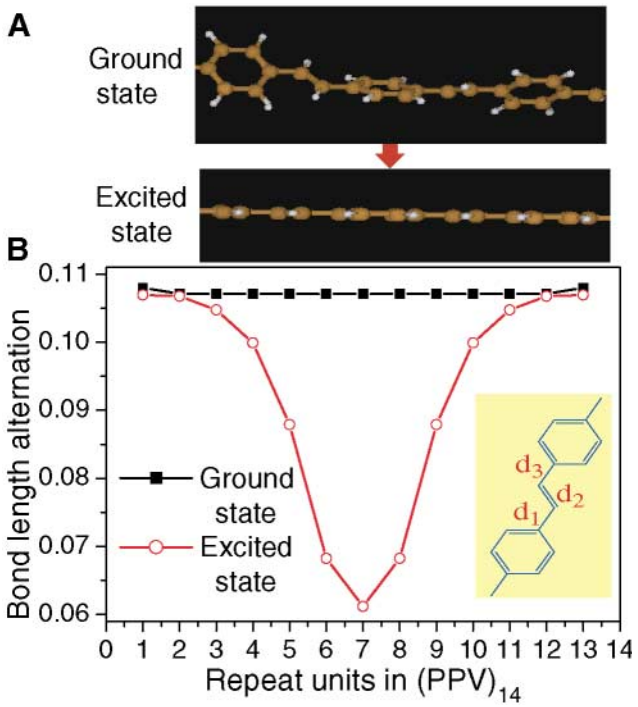

FIG. 2 (color). Geometry relaxation along the excited state surface from the ground to the lowest excited state equilibrium geometry of $(PPV)_{14}$ oligomer. The excited state structure shows reduced torsional disorder (planar geometry) (a) and reduced bond-length alternation $\frac{d_1+d_3}{2} - d_2$ in the middle of the molecule (b), as compared to the ground-state geometry.

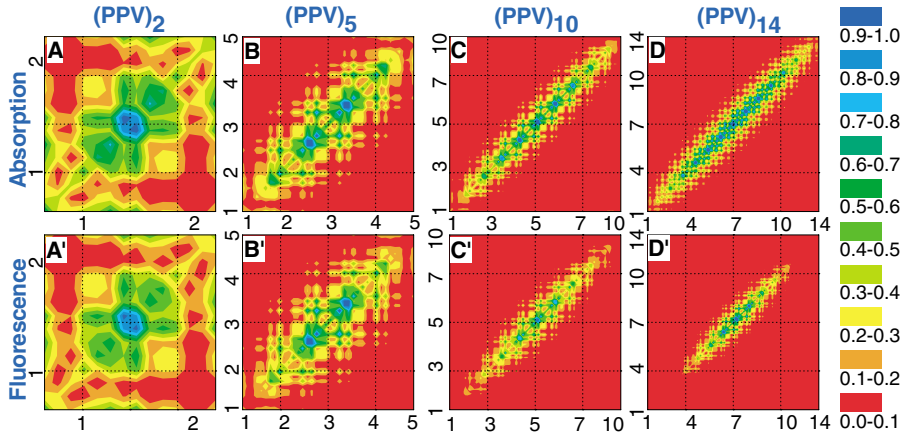

FIG. 3 (color). Contour plots of transition density matrices. (a)–(d) represent transition from the ground state (equilibrium geometry) to the lowest excited state in $(PPV)_2$, $(PPV)_5$, $(PPV)_{10}$, and $(PPV)_{14}$ oligomers, respectively, and correspond to vertical absorption. (a′)–(d′) are the same quantities as in (a)–(d), but computed at the excited state equilibrium geometries and correspond to vertical fluorescence. The axes labels represent the number of repeat units, and the color code is shown in the bottom panel.

geometry. Karabunarliev and co-workers reported similar trends in smaller PPV oligomers ($n = 2$–6) studied with a limited CI/AM1 method [15].

To investigate how these geometrical changes are connected with the underlying photoinduced dynamics of electronic charges, we further use two-dimensional real-space analysis of transition densities, representing the electronic transition between the ground state and an electronically excited state [9,10]. Photoexcitation creates an electron-hole pair or an exciton by moving an electron from an occupied orbital to an unoccupied orbital. Each element of the transition density reflects the dynamics of this exciton projected on a pair of atomic orbitals given by its indices. A detailed real-space analysis of characteristic electronic excitations of PPV oligomers is given in [9].

Plots of transition density matrices in PPV oligomers are shown in Fig. 3. Each plot depicts probabilities of an electron moving from one molecular position (horizontal axis) to another (vertical axis), under a transition from the ground state to the $1B_u$ excited state. An electron-hole pair initially created by an absorbed photon (“hot exciton”) is entirely delocalized in the smallest oligomer $(PPV)_2$ and confined by the molecular ends [Fig. 3(a)]. For longer oligomers [Figs. 3(c) and 3(d)], the electron-hole pair is also delocalized over the whole chain (diagonal in the plot) but is not confined by the molecular ends. The exciton size (maximal distance between electron and hole) is four repeat units (largest off-diagonal extent of the nonzero matrix area). This electronic excitation then relaxes along the excited state potential surface into a “cold exciton,” which may decay radiatively back to the ground state (fluorescence). Figures 3(a′)–3(d′) display corresponding transition densities computed in the excited state geometry. Transition densities in the ground- and excited state geometries in the smaller oligomers $(PPV)_2$ and $(PPV)_5$, being in the confined regime, are very similar, as seen from comparing plots Figs. 3(a) and 3(a′) [3(b) and 3(b′)]. However, the effect of the excited state geometry relaxation is clearly observed for longer oligomers [$(PPV)_{10}$ and $(PPV)_{14}$] by comparing plots Figs. 3(c) and 3(c′) [3(d) and 3(d′)]: the exciton, initially diagonally delocalized along the whole molecule, becomes localized in the center of the chain. We notice that relaxed excitations in $(PPV)_{10}$ [plot 3(c′)] and $(PPV)_{14}$ [plot 3(d′)] are virtually identical, with a diagonal size of about six repeat units in the middle of the molecule, consistent with the region of reduced bond-length alternation in Fig. 2(b). This suggests exciton self-trapping [6] at the center of the chain by vibrational relaxation.

Finally, a direct comparison with experiment may be drawn by computing photoluminescence spectra in the zero temperature limit using the ground- and excited state optimal geometries. The probability of emission from

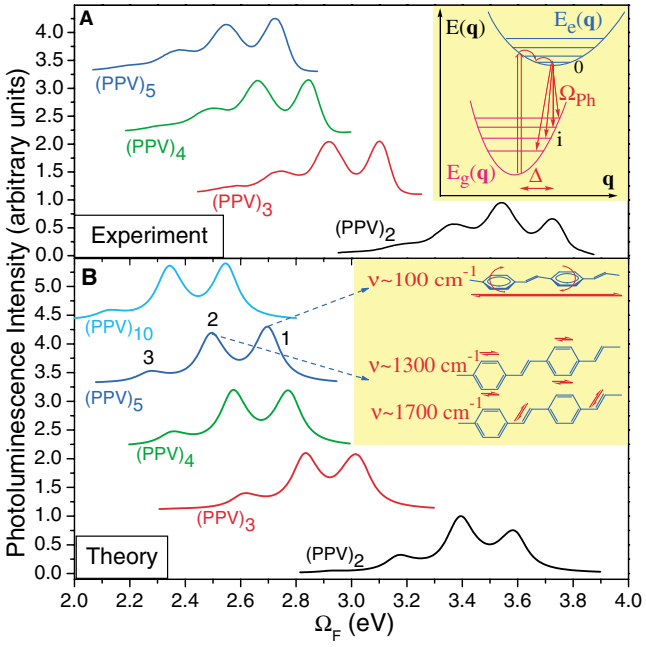

FIG. 4 (color). Experimental (a) [21] and calculated (b) photoluminescence spectra of PPV oligomers. Inset in (a) schematically displays emission processes between vibrational levels of the excited and ground states controlled by magnitudes of corresponding Franck-Condon factors. Inset in (b) shows dominant nuclear motions leading to vibrational structure of the fluorescence line shape.

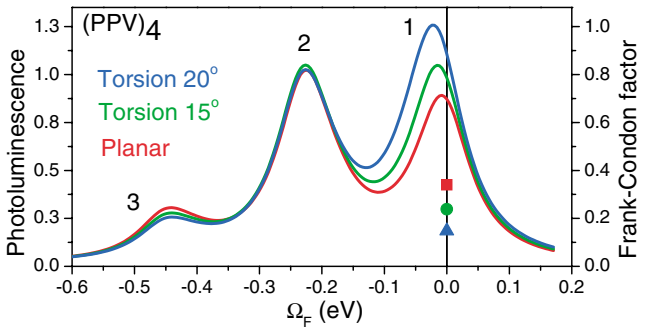

FIG. 5 (color). Variation of fluorescence line shape vibrational structure and corresponding Franck-Condon factors for 0-0 transition (colored symbols) with torsional angle calculated for $(PPV)_4$. The energy of the 0-0 transition is shifted to 0.0 for each of them. There is a moderate blueshift in the absolute transition energies as a function of increasing torsional angle. The intensity of peak 2 is normalized to unity for all three curves.

transition between the vibrational level 0 in the lowest excited state and a vibrational level i in the ground state [inset, Fig. 4(a)] depends on the magnitude of the corresponding Franck-Condon overlap, which in turn is related to the displacement Δ along the ground-state vibrational mode describing the geometry deformation in the excited state [15,21]. This approach does not consider the effects of Dushinsky rotation in the excited state. We believe this is justified, as we are concerned with the assignment of fairly broad spectral features, and the typical redistribution of intensities caused by Dushinsky rotation should not affect our conclusions. The spectra calculated for PPV oligomers shown in Fig. 4(b) closely resemble the experimental spectra [Fig. 4(a)] and are very similar to spectra computed with the limited CI/AM1 method [15]. Further analysis of characteristic nuclear motions strongly contributing to Franck-Condon overlaps attributes peak 1 [Fig. 4(b)] to the 0-0 transition and slow vibrational motions corresponding to torsional twisting and chain stretching smeared by broadening (a linewidth of 0.05 eV [21] has been used in calculations) into one peak; in contrast, peak 2 and its overtone peak 3 are mediated by fast vibrational modes such as the C═C stretch and quinoidal motions of phenyls [inset, Fig. 4(b)]. These are two typical geometry deformations we observed in the course of excited state relaxation (Fig. 2). In particular, increasing torsional angle leads to larger displacements in the slow vibrational motions, which in turn enhance the overall intensity of peak 1, even though the probability of the 0-0 transition is reduced, as illustrated in Fig. 5. This suggests that the ratio between intensities of photoluminescence peaks depends on the morphology of the PPV material (Fig. 5) and could be observed experimentally [22,23].

In conclusion, we have studied relaxation of the lowest excited state surface in PPV oligomers using a new approach for simulation of the excited state molecular dynamics. The analysis identified vibrational motions strongly coupled to the electronic structure and accompanying the relaxation of the initial photoexcitation on the excited state surface. This leads to confinement of the electronic excitation over about six repeat units (self-trapped exciton formation). The computed photoluminescence spectra are related to specific slow and fast nuclear motions and agree well with experiment. Observed trends correlate well with conclusions derived from modeling experimental photoluminescence spectra [21].

This work was performed under the auspices of the U.S. Department of Energy. The authors thank Dr. E. Tsiper, Dr. A. Piryatinski, and Dr. M. Chertkov for their critical comments.

*Corresponding author.
Email address: serg@lanl.gov

[1] M. A. Baldo, M. E. Thompson, and S. R. Forrest, Nature (London) **403**, 750 (2000); R. H. Friend *et al.*, Nature (London) **397**, 121 (1999).
[2] X. Hu *et al.*, Proc. Natl. Acad. Sci. USA **95**, 5935 (1998); F. Gai *et al.*, Science **279**, 1886 (1998).
[3] J. L. Brédas *et al.*, Acc. Chem. Res. **32**, 267 (1999).
[4] F. C. Spano, Chem. Phys. Lett. **331**, 7 (2000).
[5] A. Kohler *et al.*, Nature (London) **392**, 903 (1998).
[6] A. J. Heeger *et al.*, Rev. Mod. Phys. **60**, 781 (1988).
[7] R. Osterbacka *et al.*, Science **287**, 839 (2000).
[8] F. Molnar *et al.*, J. Mol. Structure Theochem. **506**, 169 (2000).
[9] S. Mukamel *et al.*, Science **277**, 781 (1997); S. Tretiak *et al.*, J. Phys. Chem. B **104**, 7029 (2000).
[10] S. Tretiak, V. Chernyak, and S. Mukamel, J. Phys. Chem. B **102**, 3310 (1998).
[11] E. V. Tsiper *et al.*, Chem. Phys. Lett. **302**, 77 (1999); E. V. Tsiper *et al.*, J. Chem. Phys. **110**, 8328 (1999).
[12] M. Tommasini *et al.*, J. Phys. Chem. A **105**, 7057 (2001).
[13] M. J. S. Dewar *et al.*, J. Am. Chem. Soc. **107**, 3902 (1985).
[14] S. Tretiak *et al.*, Chem. Phys. Lett. **331**, 561 (2000); S. Tretiak *et al.*, J. Chem. Phys. **115**, 699 (2001).
[15] S. Karabunarliev *et al.*, J. Chem. Phys. **113**, 11372 (2000); S. Karabunarliev *et al.*, J. Phys. Chem. A **104**, 8236 (2000).
[16] M. P. Allen and D. J. Tildesley, *Computer Simulation of Liquids* (Clarendon Press, Oxford, 1987).
[17] E. R. Davidson, J. Comput. Phys. **17**, 87 (1975); R. E. Stratmann, G. E. Scuseria, and M. J. Frisch, J. Chem. Phys. **109**, 8218 (1998).
[18] S. J. Martin *et al.*, Opt. Mater. **9**, 88 (1998).
[19] P. F. can Hutten *et al.*, J. Am. Chem. Soc. **121**, 5910 (1999).
[20] S. R. Marder *et al.*, Science **263**, 511 (1994).
[21] J. Cornil *et al.*, Chem. Phys. Lett. **278**, 139 (1997); J. Cornil *et al.*, Chem. Phys. Lett. **247**, 425 (1995).
[22] P. K. H. Ho *et al.*, J. Chem. Phys. **115**, 2709 (2001); T. W. Hagler *et al.*, Phys. Rev. B **44**, 8652 (1994).
[23] J. Yu, D. H. Hu, and P. F. Barbara, Science **289**, 1327 (2000).